Published in final edited form as:
*Gene Ther*. 2008 July ; 15(14): 1024–1034. doi:10.1038/gt.2008.30.

# Heat shock protein inhibitors increase the efficacy of measles virotherapy

**C Liu**[1], **C Erlichman**[2], **CJ McDonald**[1], **JN Ingle**[2], **P Zollman**[1], **I Iankov**[1], **SJ Russell**[1], and **E Galanis**[1,2]

[1]Department of Molecular Medicine, Mayo Clinic, Rochester, MN, USA

[2]Division of Medical Oncology, Mayo Clinic, Rochester, MN, USA

## Abstract

Oncolytic measles virus strains have activity against multiple tumor types and are currently in phase I clinical testing. Induction of the heat shock protein 70 (HSP70) constitutes one of the earliest changes in cellular gene expression following infection with RNA viruses including measles virus, and HSP70 upregulation induced by heat shock has been shown to result in increased measles virus cytotoxicity. HSP90 inhibitors such as geldanamycin (GA) or 17-allylaminogeldanamycin result in pharmacologic upregulation of HSP70 and they are currently in clinical testing as cancer therapeutics. We therefore investigated the hypothesis that heat shock protein inhibitors could augment the measles virus-induced cytopathic effect. We tested the combination of a measles virus derivative expressing soluble human carcinoembryonic antigen (MV-CEA) and GA in MDA-MB-231 (breast), SKOV3.IP (ovarian) and TE671 (rhabdomyosarcoma) cancer cell lines. Optimal synergy was accomplished when GA treatment was initiated 6–24 h following MV infection. Western immunoblotting confirmed HSP70 upregulation in combination-treated cells. Combination treatment resulted in statistically significant increase in syncytia formation as compared to MV-CEA infection alone. Clonogenic assays demonstrated significant decrease in tumor colony formation in MV-CEA/GA combination-treated cells. In addition there was increase in apoptosis by 4,6-diamidino-2-phenylindole staining. Western immunoblotting for caspase-9, caspase-8, caspase-3 and poly(ADP-ribose) polymerase (PARP) demonstrated increase in cleaved caspase-8 and PARP. The pan-caspase inhibitor Z-VAD-FMK and caspase-8 inhibitor Z-IETD-FMK, but not the caspase-9 inhibitor Z-IEHD-FMK, protected tumor cells from MV-CEA/GA-induced PARP activation, indicating that apoptosis in combination-treated cells occurs mainly via the extrinsic caspase pathway. Treatment of normal cells, such as normal human fibroblasts, however, with the MV-CEA/GA combination, did not result in cytopathic effect, indicating that GA did not alter the MV-CEA specificity for tumor cells. One-step viral growth curves, western immunoblotting for MV-N protein expression, QRT-PCR quantitation of MV-genome copy number and CEA levels showed comparable proliferation of MV-CEA in GA-treated vs -untreated tumor cells. Rho activation assays and western blot for total RhoA, a GTPase associated with the actin cytoskeleton, demonstrated decrease in RhoA activation in combination-treated cells, a change previously shown to be associated with increase in paramyxovirus-induced cell—cell fusion. The enhanced cytopathic effect resulting from measles virus/GA combination supports the translational potential of this approach in the treatment of cancer.



Correspondence: Dr E Galanis, Mayo Clinic, 200 First Street SW, Rochester, MN 55905, USA. E-mail: galanis.evanthia@mayo.edu.

Supplementary Information accompanies the paper on Gene Therapy website (http://www.nature.com/gt)

**Keywords**

measles; virotherapy; GA; heat shock protein inhibitors; RhoA

## Introduction

Measles virus is a negative-strand RNA virus that belongs to the family of Paramyxoviridae.1 Antitumor activity of attenuated strains of measles virus derived from the Edmonston vaccine lineage has been demonstrated in models of lymphoma,2 multiple myeloma,3 ovarian cancer,4 hepatocellular carcinoma,5 glioblastoma multiforme6 and breast cancer.7 After infection of tumor cells, the virus causes a very characteristic cytopathic effect, the development of multinucleated giant cells (syncytia). Infected cells express the viral hemagglutinin (H) and fusion (F) proteins on their membranes thereby become highly fusogenic, causing fusion with uninfected neighboring cells.

Measles virus infection-induced stress response is characterized by an increase in both cytosolic and endoplastic reticulum luminal molecular chaperones.8 Induction of heat shock protein 70 (HSP70) is one of the earliest indications of cellular stress following infection with both RNA and DNA viruses. Furthermore, HSP70 upregulation induced by heat shock has been shown to result in increase in measles virus-induced cytopathic effect.9-11

Heat shock protein inhibitors such as geldanamycin (GA) target heat shock protein 90 (HSP90),12,13 one of the most highly conserved members of the cellular chaperone machinery, by binding competitively to its N-terminal ATP-binding site, and causing the degradation of multiple client proteins through the ubiquitin—proteasome pathway, which leads to cell cycle arrest and apoptosis.14 GA has been shown to be cytotoxic and/or cytostatic against multiple tumor cell lines *in vitro*.9,15 Although GA can cause animal toxicity *in vivo*, better tolerated analogs such as 17-allylaminogeldanamycin (17-AAG) have resulted in *in vivo* antitumor activity in breast, melanoma and ovarian mouse xenograft models.16-18 Phase I trials of 17-AAG have been completed.19,20

Given the fact that heat shock protein-targeting agents result in upregulation of HSP70 and the latter, when induced by heat shock, has been associated with increase in measles virus cytopathic effect, we hypothesized that combination of oncolytic measles virus derivatives with heat shock protein inhibitors can increase the efficacy of MV virotherapy.

Our experiments showed that the combination of measles virus derivatives with heat shock protein inhibitors can enhance the cytopathic and antitumor effect of measles virotherapy, and increase virus-induced apoptosis. Since both measles virus derivatives and heat shock protein inhibitors are currently in clinical testing, those findings could have translational implications in the treatment of cancer patients.

## Results

### GA significantly increases measles virus-induced CPE in vitro

In optimization experiments we assessed the antiproliferative effect of GA in a variety of tumor cell lines. The lowest concentration of GA (30 $n_M$), which was associated with upregulation of HSP70, but had minimal cytopathic effect, was used in subsequent combination experiments. The following sequences were examined: (1) 6 or 24 h of GA treatment followed by infection with a measles virus derivative expressing soluble human carcinoembryonic antigen (MV-CEA); (2) MV-CEA infection followed 24 h later by GA treatment and (3) GA and MV-CEA administered concomitantly. Crystal violet staining was

performed at multiple time points from 24 to 76 h to examine the effect of all combination treatments. The addition of GA increased the cytopathic effect of MV-CEA, independent of the sequence combination (data not shown). However, the effect was more prominent when GA treatment was initiated 24 h following MV infection. This effect was observed in different tumor cell lines (Figure 1a), including MDA-MB-231 (breast), SKOV3.ip (ovarian) and TE671 (rhabdomyosarcoma) at different multiplicities of infection (MOIs) of MV-CEA from 0.01 to 1. When normal cell lines such as normal human dermal fibroblasts (NHDFs), which do not fuse after measles virus infection, were treated with the GA/MV combination, no cytopathic effect was observed, indicating that GA does not alter the selectivity of MV for tumor cells, and does not increase fusogenicity of MV in no transformed lines (Figure 1b). Quantitation of the syncytial size showed statistically significant increase of the syncytial area in the measles virus infection followed by GA treatment group, as compared to single-agent measles virus treatment (Figure 1c).

### MV-CEA/GA combination treatment increased antitumor effect in vitro

To examine the impact of MV-CEA/GA combination treatment on cell survival, clonogenic assays were employed. Figures 2a and b show representative results in MDA-MB231 and SKOV3.IP cells. There was significant decrease in colony formation in MV-CEA/GA group as compared to either single-agent MV-CEA alone at comparable MOIs, or single-agent GA (30 $n_M$) in both cell lines, indicating that combination treatment significantly increases the antitumor effect of MV-CEA virotherapy. The $IC_{50}$ for MD-MB231 cells and SK0V3.IP cells treated with MV-CEA/GA were MOIs of 0.20 and 0.34, respectively, whereas MV-CEA alone did not achieve an $IC_{50}$ in either cell line up to the MOIs tested.

### MV/GA combination increases tumor cell apoptosis, which is mainly mediated via activation of the extrinsic caspase pathway

We have previously demonstrated that measles infection results in tumor cell apoptosis.6,7 We explored the hypothesis that the MV-CEA/GA combination treatment increases the antitumor effect by promoting an increase in apoptosis. DAPI (4,6-diamidino-2-phenylindole) staining was employed to quantify the number of apoptotic cells in MV/GA-treated cancer cells. Cell fusion was inhibited by pretreatment with FIP to allow better quantification of apoptotic cells. The number of apoptotic cells, identified by condensation and fragmentation of the nuclei was significantly increased in both MV-CEA-(MOI 1.0) and MV-CEA/GA-treated groups as compared to either GA (30 $n_M$) alone or untreated controls. In addition, the percentage of apoptotic cells was significantly higher in the MV-CEA/GA-treated group, as compared to the MV-CEA group ($P$=0.02) (Figure 3a). To further investigate the mechanism of MV-CEA/GA-caused apoptosis, western blot analysis for caspase-8, -9, -3 and poly(ADP-ribose) polymerase (PARP) (p85) in MV/GA-treated MDA-MB231 cells were performed. Increased cleavage of caspase-8, and PARP were observed in MV-CEA/GA combination-treated cells as compared to single-agent MV-CEA (MOI 1.0), single-agent GA (30 $n_M$) or untreated control cells (Figure 3b). However, there was little difference in activation of caspase-9. We also examined the inhibitory effect of caspase inhibitors on PARP cleavage. There was complete inhibition of PARP cleavage in MV-CEA/GA-treated cells after the addition of pan-caspase or caspase-8 inhibitor, but not caspase-9 inhibitor, indicating that activation of apoptosis in combination-treated cells is mostly mediated via the extrinsic caspase pathway (Figure 3c).

### MV-CEA/GA combination treatment results in increase in HSP70 levels that is comparable to single-agent GA

GA is a specific inhibitor of HSP90, and GA treatment caused HSP90 suppression as well as increased HSP70 expression.12,14 Measles virus infection has been reported to upregulate

expression of HSP70 and the increased HSP70 could play an important role in MV-caused cytopathic effect.9,10 HSP70 and HSP90 protein levels in response to treatment with MV-CEA, GA and the combination were examined by western immunoblotting. Inducible HSP70 levels were increased by GA alone and when combined with MV. The increase seen with the combination was the same as with GA alone (Figure 4). The lack of GA effect on HSP90 reflects the detection of both the constitutively expressed and the inducible forms of the protein by the antibody used.

## Increased syncytial formation in MV-CEA/GA combination-treated cells is not due to increased viral proliferation

By employing fluorescence-activated cell sorting (FACS) analysis, we demonstrated that treatment with GA does not alter the expression on measles virus receptor CD46 on tumor cells (Figure 5a), or normal cells, and therefore it does not affect viral entry. To assess if increased viral proliferation is responsible for the increase in syncytia formation and increased cytopathic effect in MV-CEA/GA combination-treated cells, one-step viral growth curves were performed. As shown in Figure 5b, GA treatment did not significantly change the growth kinetics of MV-CEA in either MDA-MB-231 or SKOV3.IP cells. To further confirm this, QRT-PCR to assess viral genome copy number and western immunoblotting to assess expression of the viral N-protein were performed. There was no significant difference in viral genome copy number or viral protein expression on combination treated cells as compared to MV-CEA infection alone (Figures 5c and d). Similarly there was no difference in expression of viral F protein (Supplementary Figure 1). Furthermore CEA levels, a surrogate of viral gene expression, were comparable between GA-treated and -untreated cells following viral infection (Figure 5e).

Newly synthesized proteins including the measles virus structural proteins must fold into their native three-dimensional structures. Molecular chaperones facilitate the initial folding of proteins to their native form. Translocation of proteins into the endoplasmic reticulum (ER) and their folding also relies on molecular chaperones associated with the ER. HSP70, the chaperone protein upregulated following treatment with GA, plays a key role in this process.21-24 We therefore investigated if the observed increase in cytopathic effect was due to upregulation of the measles H protein expression on the cell surface. Immunoblotting of cell surface-biotinylated proteins immunoprecipitated with an anti-FLAG antibody showed no evidence of increased H expression in combination-treated cells. In contrast the results were suggestive of decreased surface H expression (Figure 5f).

These results collectively indicate that the increased cell fusion and CPE caused by GA in combination with MV-CEA is not due to increase in viral proliferation.

## MV-CEA/GA treatment is associated with decrease in RhoA activation

To further explore the mechanism of increased syncytia formation in MV-CEA/GA-treated tumor cells, we examined the impact of combination treatment on RhoA activity. RhoA is one of the major regulators of actin cytoskeleton, and its inactivation has been associated with increase in paramyxovirus-induced fusion.25 GA has been previously shown to inhibit RhoA activation.26 Western immunoblotting was performed following immunoprecipitation to assess active RhoA expression. The results showed gradual decrease of RhoA activity starting at 6 h following GA treatment with RhoA activity becoming undetectable at 12 h after GA treatment (36 h post-MV-CEA infection). The total RhoA levels did not change significantly in all groups at any time points (Figure 6). This time course, which is consistent with the peak cytopathic effect observed in combination-treated cells supports that GA-induced RhoA inactivation increases syncytial formation and measles-induced cytopathic effect.25

### Transduction of tumor cells with dominant-negative RhoA increases measles-induced fusion

In order to further confirm that loss of RhoA activity can increase measles-induced fusion, we constructed lentiviral vectors expressing either constitutively active or dominantly negative RhoA. Transduction of MDA-MB-231 cells with a lentiviral vector expressing a dominant-negative RhoA (PHR-NegRhoA) resulted in lack of active RhoA as assessed by immunoprecipitation (Figure 6b), and significantly increased fusion following infection with measles virus (6C). The latter was confirmed with quantitation of the syncytial area (6D). There was significant increase in measles infection-induced syncytia following transduction with a lentiviral vector expressing dominant-negative RhoA, but not constitutively active RhoA or green fluorescent protein (GFP) (MV+PHR-NegRhoA vs MV+PHR-ActRhoA, $P$=0.0072; MV+PHR-NegRhoA vs MV+ PHR-GFP, $P$=0.0046, MV+PHR-NegRhoA vs MV=0.0162). These results collectively support that decrease in RhoA activation following treatment with the heat shock protein inhibitor GA is likely responsible for the increased syncytia formation in combination-treated cells.

## Discussion

GA is a naturally occurring ansamycin antibiotic that, along with its clinically used analog 17-AAG, have significant anticancer properties in preclinical models.27,28 These agents disrupt HSP90 association with client proteins by occupying the nucleotide-binding site of HSP90,29-31 therefore, preventing binding of HSP90 with ATP and affecting the composition of HSP90 containing multimolecular chaperone complexes.32,33 In view of evidence of activity in preclinical animal models,34,35 clinical trials involving 17-AAG have been initiated in humans.15

We have previously demonstrated oncolytic activity of measles virus strains against a variety of tumors including lymphoma,2 multiple myeloma,3 ovarian cancer,4 brain tumors, 6 breast cancer,7 hepatocellular carcinoma5 and we are currently testing the engineered measles virus strains MV-CEA and MV-NIS in three phase I/II trials against ovarian cancer, brain tumors and multiple myeloma.

Heat shock has been reported to increase the viral plaque size after measles virus infection.9 Similarly, constitutive overexpression of HSP70 has been shown to mediate large plaque formation by measles virus.10 Inhibition of HSP90 by heat shock protein inhibitors results in HSP70 upregulation.36 We, therefore, hypothesized that pharmacologic upregulation of HSP70 by employing heat shock protein inhibitors could result in the same effect; increase in viral plaque size and increase in the observed antitumor effect.

Our results confirm that combination of heat shock protein inhibitors with the measles virus at concentrations that can upregulate HSP70 resulted in increase in fusogenicity and increased cytopathic effect which translated to significant increase of the *in vitro* antitumor activity, as assessed by clonogenic assays.

Of equal importance, combination treatment did not decrease viral specificity in nontransformed cells, such as NHDF. It has been shown that selectivity of measles virus Edmonston vaccine strain derivatives against tumor cells can be explained on the basis of CD46 overexpression in tumor cells, in contrast to low expression levels in normal cells.37 The lack of CD46 receptor induction both in tumor as well as normal cells in response to GA treatment, as we have demonstrated here, could explain the selective sparing of normal cells from the cytopathic effect of MV/GA combination, despite the increased cytopathic effect in tumor cells.

Combination treatment also resulted in increase in virus-induced apoptosis in tumor cells. We have previously shown that apoptosis plays a key role in measles virus-induced cytopathic effect and cell death.6,7 Western immunoblotting for activated caspase-8, -9, -3 and PARP, as well as experiments employing pan-caspase, caspase-8 and -9 inhibitors support that activation of apoptosis in measles virus/GA combination-treated cells is mediated predominantly via the extrinsic caspase-8 pathway. The importance of the extrinsic caspase pathway in mediating apoptotic cell death has been previously demonstrated, both for other synergistic heat shock protein inhibitor combinations, such as the combination of the 17-AAG with suberoylanilide hydroxamic acid,38 as well as for synergistic measles virus combinations, such as the combination of the virus with external beam radiation therapy.39

We hypothesized that the observed increase in fusion in combination-treated cells is due to changes in the actin cytoskeleton, which could make cells more susceptible to fusion. Actin cytoskeleton has been shown to play an important role in virus-induced cell—cell fusion. 40,41 RhoA, a member of Rho family of GTPases and one of major regulators of actin cytoskeleton, appears to be an important regulator of cell fusion by controlling the stress fiber formation and actin rearrangement on the plasma membrane.42,43 RhoA cycles between active GTP-bound and inactive GDP-bound forms through nucleotide exchange and intrinsic GTPase activity. The active form is located on the plasma membrane, and the inactive form, in the cytosol.44 RhoA activation has been shown to affect cell fusion and syncytia formation after infection with paramyxoviurses such as respiratory syncytia virus45 and Hendra virus.25 RhoA is regulated by heat shock proteins: HSP90 is required for RhoA activation in thrombin-induced signaling to cytoskeleton, and the activation of RhoA could be specifically inhibited by GA in this reaction.26 Furthermore, RhoA co-precipitates with HSP70.46 Although there is no information regarding the role of RhoA in measles-induced fusion, because of its regulation by heat shock proteins and its role in fusion induced by other paramyxoviruses we hypothesized that changes in RhoA activity could explain the observed augmentation of fusion and cytopathic effect. Indeed, western immunoblotting confirmed decrease in RhoA activity following combination treatment. Furthermore, transduction of tumor cells with a lentivirus encoding a dominant-negative RhoA significantly increased measles-induced fusion. This novel finding supports that regulation of cytoskeleton by RhoA plays an important role in measles-induced fusion, and that decrease in active RhoA following GA treatment is likely responsible for the increased measles-induced cytopathic effect in response to combination treatment. Inactive RhoA could facilitate MV-CEA-induced cell fusion by inhibiting cortical actin (stress fiber) formation, the latter thought to stabilize the cell membrane, and by inhibiting RhoA-promoted membrane retraction: a protruding cellular membrane could be more susceptible to fusion.47

GA treatment at the low concentrations employed in our study had no impact on viral propagation. There was no difference in viral propagation between measles alone or combination-treated cells. Similarly, there was no difference in viral genome copy numbers as assessed by QRT-PCR, expression of viral H and N proteins in whole cell lysates or CEA levels. Since chaperone proteins are important for processing of the measles virus proteins through the ER complex, we also investigated the impact of GA treatment on surface expression of the viral H protein, which is the main protein responsible for receptor recognition in neighboring cells. A slight decrease of the surface H protein expression was observed in combination-treated cells, which, similarly to the other data we generated, supports that increase in viral propagation is not responsible for the observed increase in cytopathic effect.

HSP70 expression also induced by heat shock has been found to result in increased measles virus gene expression,10,11 syncytia formation and neurovirulence.48 The difference between these previous reports and our study as it pertains to viral replication can possibly be explained because of the different mechanism of HSP70 upregulation. In our study, HSP70 upregulation is due to HSP90 inhibition. The latter has been associated with suppression of replication of RNA viruses such as HCV49 and paramyxoviruses.50

Heat shock protein inhibitor/measles virus combination treatment could have additional advantages, since HSP70 induction in the tumor environment by GA or other heat shock protein inhibitors has the potential to result in augmentation of antitumoral immune response. HSP70 induction has been shown to increase lysability of tumor cells by cytotoxic T lymphocytes, without interfering with MHC class I expression and antigen presentation.51 HSP70 can also function as an immunostimulatory cytokine, activating nuclear factor-κb and upregulating the expression of proinflammatory cytokines such as tumor necrosis factor-α, interleukin (IL)-1β and -6 in human monocytes.52 It is therefore possible that tumor oncolysis in the context of heat shock protein-induced HSP70 upregulation can augment antitumor immunity and thus further increase the antitumor activity of this approach.

In summary, the combination of MV-CEA and GA treatment resulted in significant increase of the cytopathic effect against a variety of tumor cell lines, by resulting in increased syncytia formation and tumor cell apoptosis, without decreasing specificity against normal cells. These findings could have important translational implications in measles virotherapy of solid tumor.

## Materials and methods

### Cell culture and antibodies

MDA-MB-231, SKOV3.IP, TE671 and NHDF cells were obtained from ATCC and cultured according to the ATCC specifications. Antibodies used included the following: anti-measles N-protein antibody (Chemicon Mab 8906, Temecula, CA, USA), measles anti-H and anti-F antibodies (kindly provided by Dr Roberto Catanneo, Mayo Clinic), anti-RhoA (no. sc-418; Santa Cruz, Santa Cruz, CA, USA), anti-pRhoA (no. sc-32954-R; Santa Cruz), anti-caspase-3 (no. IMG-144A; IMGENEX, San Diego, CA, USA), anti-HSP70 (mouse monoclonal, no. SPA-810; Stressgen, Ann Arbor, MI, USA), anti-HSP90 (mouse monoclonal, kindly provided by Dr David Toft, Mayo Clinic), anti-caspase-8 (no. 9746; Cell Signaling, Danvers, MA, USA), anti-cleaved caspase-8 (no. 9749; Cell Signaling), anti-caspase-9 (no. 05–572; Upstate, Lake Placid, NY, USA) and anti-PARP p85 fragment pAb (no. G7341; Promega, Madison, WI, USA).

### Viral production

The measles virus derivative MV-CEA was employed for this study. This virus derives from the Edmonston-NSe strain and has been engineered to express the soluble extracellular N-terminal domain of human carcinoembryonic antigen (MV-CEA). Construction and characterization of the virus have been previously described.53 When the virus replicates, CEA expression represents a good surrogate of viral gene expression. Virus was propagated in Vero cells and its titer was determined by 50% endpoint dilution assay as previously described.6

**Measles infection and drug treatment—**Cells were plated at a density of $1\times10^6$ per well in six-well plates. The following combination sequences were tested: (1) 6 or 24 h of GA treatment followed by MV-CEA infection; (2) MV-CEA infection followed 24 h later by GA treatment and (3) GA and MV-CEA administered concomitantly. For these

experiments different viral MOIs of 0.01–1 were employed. Virus was diluted in Opti-MEM. Infection was carried out at 37 °C, and 2 h later the viral supernatant was removed and replaced with growth medium. Two different GA concentrations were tested: 10 and 30 $n_M$. MV-CEA infection followed by GA treatment 24 h later proved to be the combination associated with the highest cytopathic effect and was employed in subsequent experiments.

Following treatment, cells were fixed with 0.5% gluteraldehyde in phosphate-buffered saline (PBS) at the designated time points, and stained with crystal violet. At the same time points, cell lysates were collected for western immunoblotting and RNA was isolated for reverse transcription (RT)-PCR (or QRT-PCR) analysis.

**Syncytial index—**MDA-MB-231 cells were infected with MV-CEA at MOI 0.1 or 1. After 24 h GA (30 $n_M$) was added. Cells were fixed and crystal violet stained at 34, 37, 40 and 44 h post-MV-CEA infection. Quantitation of the syncytial surface per plate (Syncytial Index) was analyzed using NIH software.37

**Determination of CD46 expression levels—**One million tumor or NHDF cells were harvested before and at 24, 48 and 72 h after GA treatment, washed and then incubated with fluorescein isothiocyanate-labeled mouse anti-human CD46 (PharMingen, San Jose, CA, USA). Washed cells were fixed in PBS containing 0.5% paraformaldehyde and analyzed on a Becton Dickinson FACScan Plus cytometer. Analysis was performed using the CellQuest software (BD Biosciences).

**One-step viral growth curves and virus yield—**Virus titers of MV-CEA in infected tumor cells after single-agent or combination treatment were determined by one-step growth curve as previously described.6 Cells were plated into six-well plates at a density of $1\times10^6$ cells per well and 24 h later were infected with MV-CEA at an MOI of 1.0. After 24 h GA (30 $n_M$) was added and cells were harvested at 30 and 50 h after the MV infection. At the same time points, medium was collected for CEA determination. Virus was released by two cycles of freeze/thawing. Viral titers were determined on Vero cells by limiting dilution assay as previously described.6

**Clonogenic assays—**Cells were plated in six-well plates at a density of $1\times10^6$ cells per well and 24 h later were infected with MV-CEA as described. Twelve hours after the MV-CEA infection, the cells were passed into six-well plates at a density of 500 cells per well (MDA-MB-231 cells) or 300 cells per well (SKOV3.IP cells). GA (30 $n_M$) was added 72 h later. Cells were incubated at 37 °C with 5% of $CO_2$ for 10–14 days, and then the cells were fixed with 0.5% glutaraldehyde and stained with 0.025% crystal violet. Each treatment condition was tested in three replicate wells, and each experiment was repeated twice. Colonies consisting of >50 cells were counted and the colony formation for each treatment was calculated in relation to values obtained from untreated control cells as previously described.39,54

**DAPI staining—**Cells were plated onto four-well chamber slides at a density of $2\times10^5$ cells per well and incubated for 24 h in growth medium. Cells were infected with MV-GFP in opti-MEM at MOI 1.0 for 2 h and then the medium was changed to growth medium with 40 μg/ml of fusion inhibitory peptide (FIP, Bachem H-9430) to prevent measles virus-induced cell-to-cell fusion.55 Twenty-four hours after MV infection, 30 $n_M$ of GA was added to the culture for another 36 h. For DAPI staining,56 the cells were fixed with 4% paraformaldehyde for 10 min at 37 °C and then washed with PBS and stained with 4′,6-diamidino-2-phenylindole (DAPI, Inc. H-1200; Vector Laboratories, Burlingame, CA, USA). The slides were visualized and photographed by confocal microscope. DAPI-stained

nuclei were counted in three random fields per treatment with >200 cells in each field. Apoptotic cells were identified by condensation and fragmentation of the nuclei.

**Western blotting—**Cells were plated into six-well plates at a density of $1\times10^6$ cells per well and 24 h later were treated with MV-CEA/GA as described. In experiments with caspase inhibitors, cells were infected with MV-CEA in Opti-MEM at MOI 1.0 for 2 h and then the medium was changed to growth medium containing the pan-caspase inhibitor Z-VAD-FMK (Promega), caspase-8 inhibitor Z-IETD-FMK (Calbiochem, Gibbstown, NJ, USA) or caspase-9 inhibitor Z-IEHD-FMK (Calbiochem) at a concentration of 100 μm. GA (30 nM) was added 24 h later and cells were harvested at 30 and 50 h after the MV infection. Cell lysates were collected at multiple time points as previously described. Following SDS—polyacrylamide gel electrophoresis (PAGE) electrophoresis, the proteins were transferred to nitrocellulose membrane in transfer buffer (200 mM glycine, 25 mM Tris-base) at 400 mAmp. The membrane was blocked for 1 h in Tris Buffered Saline with Tween 20 (TBST) with milk (40 mM sodium chloride, 20 mM Tris, 0.1% Tween20, 0.5% nonfat dry milk). Primary antibodies against measles N protein (Chemicon Mab 8906, 1:8000 diluted in incubation buffer), measles H protein, measles F protein (1:6000), HSP70, HSP90, RhoA, caspase-3-8, -9 and PARP (1:1000 diluted in incubation buffer) were incubated with the membrane at 4 °C overnight. The membrane was washed in TBST and incubated with anti-mouse horseradish peroxidase (HRP) (Pierce 1:10 000 dilution) or anti-rabbit HRP (Pierce 1:10 000 dilution) for 45 min at room temperature. Proteins were detected using Amersham's ECL detection kit.

**RhoA activation assay—**Cells were infected with MV-CEA (MOI 1.0), followed 24 h later by GA treatment (30 nM). Cell lysates were incubated with Rhotekin-RBD beads (Cytoskeleton, Inc., Denver, CO, USA). The beads pulldown part (active RhoA) and original cell lysates (total RhoA) were probed with anti-RhoA antibody for western blot analysis.57

### Detection of surface MV-H protein expression

The MV-Hflag virus was kindly provided by Dr T Nakamura and used for these experiments.55 This virus has the same MV-NSe backbone as MV-CEA but also displays an N-terminal FLAG tag (DYKDDK), which facilitates detection by western immunobloting. MDA-MB231 cells were plated onto six-well plates at $4\times10^5$ cells per well and treated with MV-Hflag/GA as described above. The cells were washed twice with PBS after 34 h of infection and biotinylated with a Cellular Labeling kit (no. 1647652; Roche). Biotin-7-NHS stock solution (250 μl of biotinylation buffer and 1.25 μl) was added to each well sequentially and were incubated for 15 min at room temperature; 12.5 μl of stop solution was added and incubated for 15 min at room temperature. After twice washing with PBS, 500 μl of cell lysis buffer (50 mM Tris, pH 7.5, 1% (v/v) Igepal CA-630 (Sigma, St Louis, MO, USA), 1 mM EDTA, 150 mN NaCl, protease inhibitor cocktail (Sigma)) was added and the cells were collected, sonicated with 3×30 s pulses on ice and centrifuged at 12 000 *g* for 10 min at 4 °C. The supernatants were collected as cell lysates. In total 50 μl protein A beads and 1 μl anti-FLAG M2 antibody (F-3165; Sigma) were added to 350 μl of the lysates, and incubated over night at 4 °C with rotation. After washed as per the manufacturer's instructions, the beads were resuspended with 50 μl of loading buffer and boiled for 2 min at 100 °C and the sample was separated on 7.5% PAGE, transferred to polyvinylidene fluoride membrane and probed with peroxidase-coupled streptavidin (no. 1550460; Roche).49

### Quantitative reverse transcription-polymerase chain reaction for detection of measles virus N-mRNA

The cDNA corresponding to the MV-CEA N gene was amplified with the primers: 5′-GAGAAGCCAGGGA GAGCTACAG-3′ (forward), 5′-GGGCAGCTCTCGCAT CAC-3′ (reverse); and the probe 5′-/56-FAM/AAACCG GGCCCAGCAGAGCAA/3BHQ_1/-3′ (Integrated DNA Technologies, Inc., Coralville, IA, USA). Standards of MV-CEA N gene was synthesized as 5′-GAGAAGCC AGGGAGAGCTACAGAGAAACCGGGCCCAGCAGA GCAAGTGATGCGAGAGCTGCCC-3′ (Dharmacon Inc., Lafayette, CO, USA) for generating the standard curves in the Q-PCR reactions. A prepared PCR master mix containing 4 $m_M$ $MgCl_2$ and 1 μg of RNA was added and run on the Stratagene MX4000 cycler with the following cycling conditions: 30 min at 45 °C, 10 min at 95 °C, 40 cycles of 60 s at 55 °C and of 15 s at 95 °C.

### Construction of lentiviral vectors expressing constitutively active RhoA (PHR-ActRhoA) and dominant-negative RhoA (PHR-neg RhoA)

Total RNA was isolated from MDA-MB231 cells using the Rneasy Mini kit (Qiagen, Miami, FL, USA), and the wild-type RhoA cDNA was amplified by RT—PCR with primers: 5′-GGATCCATGGCCATCAAGAAACTG-3′ (forward), 5′-TCACAAGACAAGGCAACCAGATTT-3′ (reverse) and the following cycling conditions, 94 °C for 30 s, 55 °C for 45 s, 72 °C for 90 s (40 cycles) and cloned into pCRII (Invitrogen, Carlsbad, CA, USA).

To generate constitutively active and dominant-negative RhoA, PCR site-directed mutagenesis of Gln→Leu at codon 6358 and Thr→Asn at codon 19 of RhoA59 was performed using PfuTurbo DNA polymerase (Stratagene, La Jolla, CA, USA) and the pCRII-RhoA as a template. The following primers were applied; RhoA-L63: 5′-GACACAGCTGGATTGGAAGATTATG-3′ (forward), 5′-CATAATCTTCCAATCCAGCTGTGTC-3′ (reverse); RhoA-N19: 5′-CCTGTGGAAAGAACTGCTTG CTCATAG-3′ (forward), 5′-CTATGAGCAAGTTCTTTCC ACAGG-3′ (reverse) and the following cycling conditions: RhoA-L63: 96 °C for 45 s, 55 °C for 45 s, 68 °C for 600 s (16 cycles), RhoA-N19: 97 °C for 45 s, 56 °C for 45 s, 68 °C for 600 s (16 cycles). The transfer vector plasmids for the RhoA-L63 Lenti and RhoA-N19 lentivectors PHR-ActRhoA and PHR-NegRhoA were constructed by replacing the GFP fragment of lentiviral vector plasmid pHR-SIN-CSGWdlNotI (kindly provided by Dr Y Ikeda, Mayo Clinic Rochester, MN, USA) with the mutated cDNAs of RhoA-L63 or RhoA-N19 fragment.

HIV-1 vectors pseudotyped with VSV.G envelopes were generated by transient transfection of 30 μg transfer vector plasmid, 30 μg pCMV8.91 gag-pol-expressing plasmid and 10 μg pMD.G (envelope vector) into 293T cells plated in T75 flasks using calcium phosphate co-precipitation method and titers were determined as previously described.3

### Assessment of impact of RhoA status on measles-induced fusion

MDA-MB231 cells were plated overnight in six-well plates ($2\times10^5$-$10^6$ cells per well) and infected with MV-GFP in opti-MEM at MOI 0.5 for 2 h at 37 °C. Media were replaced with fresh growth medium for 2 h at 37 °C, and cells were infected overnight with lentiviruses (MOI 10) in the presence of 8 μg $ml^{-1}$ polybrene. Cells were fixed and stained by crystal violet at 36 h post-MV-GFP infection. Quantification of the syncytial area (Syncytial Index) was performed using NIH software (ImageJ).37

### Statistical analysis

All quantitative data are presented as the mean±s.e.m. Comparisons between groups were performed using *t*-test. A two-sided $P \leq 0.05$ was considered statistically significant.

## Supplementary Material

Refer to Web version on PubMed Central for supplementary material.

## Acknowledgments

This work was supported by the Atwater Fund (EG); P50 CA 116201 (JNI, EG); P50 CA 108961 (EG).

## References

1. Wild TF, Malvoisin E, Buckland R. Measles virus: both the haemagglutinin and fusion glycoproteins are required for fusion. J Gen Virol. 1991; 72(Part 2):439–442. [PubMed: 1993882]
2. Grote D, Russell SJ, Cornu TI, Cattaneo R, Vile R, Poland GA, et al. Live attenuated measles virus induces regression of human lymphoma xenografts in immunodeficient mice. Blood. 2001; 97:3746–3754. [PubMed: 11389012]
3. Peng KW, Ahmann GJ, Pham L, Greipp PR, Cattaneo R, Russell SJ. Systemic therapy of myeloma xenografts by an attenuated measles virus. Blood. 2001; 98:2002–2007. [PubMed: 11567982]
4. Peng KW, TenEyck CJ, Galanis E, Kalli KR, Hartmann LC, Russell SJ. Intraperitoneal therapy of ovarian cancer using an engineered measles virus. Cancer Res. 2002; 62:4656–4662. [PubMed: 12183422]
5. Blechacz B, Splinter PL, Greiner S, Myers R, Peng KW, Federspiel MJ, et al. Engineered measles virus as a novel oncolytic viral therapy system for hepatocellular carcinoma. Hepatology. 2006; 44:1465–1477. [PubMed: 17133484]
6. Phuong LK, Allen C, Peng KW, Giannini C, Greiner S, TenEyck CJ, et al. Use of a vaccine strain of measles virus genetically engineered to produce carcinoembryonic antigen as a novel therapeutic agent against glioblastoma multiforme. Cancer Res. 2003; 63:2462–2469. [PubMed: 12750267]
7. McDonald CJ, Erlichman C, Ingle JN, Rosales GA, Allen C, Greiner SM, et al. A measles virus vaccine strain derivative as a novel oncolytic agent against breast cancer. Breast Cancer Res Treat. 2006; 99:177–184. [PubMed: 16642271]
8. Oglesbee MJ, Pratt M, Carsillo T. Role for heat shock proteins in the immune response to measles virus infection. Viral Immunol. 2002; 15:399–416. [PubMed: 12479391]
9. Parks CL, Lerch RA, Walpita P, Sidhu MS, Udem SA. Enhanced measles virus cDNA rescue and gene expression after heat shock. J Virol. 1999; 73:3560–3566. [PubMed: 10196245]
10. Vasconcelos DY, Cai XH, Oglesbee MJ. Constitutive overexpression of the major inducible 70 kDa heat shock protein mediates large plaque formation by measles virus. J Gen Virol. 1998; 79(Part 9):2239–2247. [PubMed: 9747734]
11. Vasconcelos D, Norrby E, Oglesbee M. The cellular stress response increases measles virus-induced cytopathic effect. J Gen Virol. 1998; 79(Part 7):1769–1773. [PubMed: 9680141]
12. Whitesell L, Bagatell R, Falsey R. The stress response: implications for the clinical development of hsp90 inhibitors. Curr Cancer Drug Targets. 2003; 3:349–358. [PubMed: 14529386]
13. Maloney A, Clarke PA, Workman P. Genes and proteins governing the cellular sensitivity to HSP90 inhibitors: a mechanistic perspective. Curr Cancer Drug Targets. 2003; 3:331–341. [PubMed: 14529385]
14. Scheibel T, Siegmund HI, Jaenicke R, Ganz P, Lilie H, Buchner J. The charged region of Hsp90 modulates the function of the N-terminal domain. Proc Natl Acad Sci USA. 1999; 96:1297–1302. [PubMed: 9990018]
15. Goetz MP, Toft DO, Ames MM, Erlichman C. The Hsp90 chaperone complex as a novel target for cancer therapy. Ann Oncol. 2003; 14:1169–1176. [PubMed: 12881371]
16. Price JT, Quinn JM, Sims NA, Vieusseux J, Waldeck K, Docherty SE, et al. The heat shock protein 90 inhibitor, 17-allylamino-17-demethoxygeldanamycin, enhances osteoclast formation and

potentiates bone metastasis of a human breast cancer cell line. Cancer Res. 2005; 65:4929–4938. [PubMed: 15930315]

17. Burger AM, Fiebig HH, Stinson SF, Sausville EA. 17-(allylami-no)-17-demethoxygeldanamycin activity in human melanoma models. Anticancer Drugs. 2004; 15:377–387. [PubMed: 15057143]
18. Banerji U, Walton M, Raynaud F, Grimshaw R, Kelland L, Valenti M, et al. Pharmacokinetic-pharmacodynamic relationships for the heat shock protein 90 molecular chaperone inhibitor 17-allylamino, 17-demethoxygeldanamycin in human ovarian cancer xenograft models. Clin Cancer Res. 2005; 11:7023–7032. [PubMed: 16203796]
19. Goetz MP, Toft D, Reid J, Ames M, Stensgard B, Safgren S, et al. Phase I trial of 17-allylamino-17-demethoxygeldanamycin in patients with advanced cancer. J Clin Oncol. 2005; 23:1078–1087. [PubMed: 15718306]
20. Nowakowski GS, McCollum AK, Ames MM, Mandrekar SJ, Reid JM, Adjei AA, et al. A phase I trial of twice-weekly 17-allylamino-demethoxy-geldanamycin in patients with advanced cancer. Clin Cancer Res. 2006; 12:6087–6093. [PubMed: 17062684]
21. Park SH, Bolender N, Eisele F, Kostova Z, Takeuchi J, Coffino P, et al. The cytoplasmic Hsp70 chaperone machinery subjects misfolded and endoplasmic reticulum import-incompetent proteins to degradation via the ubiquitin—proteasome system. Mol Biol Cell. 2007; 18:153–165. [PubMed: 17065559]
22. Mayer MP, Bukau B. Hsp70 chaperones: cellular functions and molecular mechanism. Cell Mol Life Sci. 2005; 62:670–684. [PubMed: 15770419]
23. Bukau B. Ribosomes catch Hsp70s. Nat Struct Mol Biol. 2005; 12:472–473. [PubMed: 15933729]
24. Hartl FU. Molecular chaperones in cellular protein folding. Nature. 1996; 381:571–579. [PubMed: 8637592]
25. Schowalter RM, Wurth MA, Aguilar HC, Lee B, Moncman CL, McCann RO, et al. Rho GTPase activity modulates paramyxovirus fusion protein-mediated cell—cell fusion. Virology. 2006; 350:323–334. [PubMed: 16500690]
26. Pai KS, Mahajan VB, Lau A, Cunningham DD. Thrombin receptor signaling to cytoskeleton requires Hsp90. J Biol Chem. 2001; 276:32642–32647. [PubMed: 11413145]
27. Whitesell L, Shifrin SD, Schwab G, Neckers LM. Benzoquinonoid ansamycins possess selective tumoricidal activity unrelated to src kinase inhibition. Cancer Res. 1992; 52:1721–1728. [PubMed: 1551101]
28. Schnur RC, Corman ML, Gallaschun RJ, Cooper BA, Dee MF, Doty JL, et al. erbB-2 oncogene inhibition by geldanamycin derivatives: synthesis, mechanism of action, and structure-activity relationships. J Med Chem. 1995; 38:3813–3820. [PubMed: 7562912]
29. Grenert JP, Sullivan WP, Fadden P, Haystead TA, Clark J, Mimnaugh E, et al. The amino-terminal domain of heat shock protein 90 (hsp90) that binds geldanamycin is an ATP/ADP switch domain that regulates hsp90 conformation. J Biol Chem. 1997; 272:23843–23850. [PubMed: 9295332]
30. Prodromou C, Roe SM, O'Brien R, Ladbury JE, Piper PW, Pearl LH. Identification and structural characterization of the ATP/ADP-binding site in the Hsp90 molecular chaperone. Cell. 1997; 90:65–75. [PubMed: 9230303]
31. Stebbins CE, Russo AA, Schneider C, Rosen N, Hartl FU, Pavletich NP. Crystal structure of an Hsp90-geldanamycin complex: targeting of a protein chaperone by an antitumor agent. Cell. 1997; 89:239–250. [PubMed: 9108479]
32. An WG, Schnur RC, Neckers L, Blagosklonny MV. Depletion of p185erbB2, Raf-1 and mutant p53 proteins by geldanamycin derivatives correlates with antiproliferative activity. Cancer Chemother Pharmacol. 1997; 40:60–64. [PubMed: 9137531]
33. Obermann WM, Sondermann H, Russo AA, Pavletich NP, Hartl FU. *In vivo* function of Hsp90 is dependent on ATP binding and ATP hydrolysis. J Cell Biol. 1998; 143:901–910. [PubMed: 9817749]
34. Solit DB, Zheng FF, Drobnjak M, Munster PN, Higgins B, Verbel D, et al. 17-allylamino-17-demethoxygeldanamycin induces the degradation of androgen receptor and HER-2/neu and inhibits the growth of prostate cancer xenografts. Clin Cancer Res. 2002; 8:986–993. [PubMed: 12006510]

35. Kelland LR, Sharp SY, Rogers PM, Myers TG, Workman P. DT-diaphorase expression and tumor cell sensitivity to 17-allylami-no, 17-demethoxygeldanamycin, an inhibitor of heat shock protein 90. J Natl Cancer Inst. 1999; 91:1940–1949. [PubMed: 10564678]
36. Whitesell L, Sutphin PD, Pulcini EJ, Martinez JD, Cook PH. The physical association of multiple molecular chaperone proteins with mutant p53 is altered by geldanamycin, an hsp90-binding agent. Mol Cell Biol. 1998; 18:1517–1524. [PubMed: 9488468]
37. Anderson BD, Nakamura T, Russell SJ, Peng KW. High CD46 receptor density determines preferential killing of tumor cells by oncolytic measles virus. Cancer Res. 2004; 64:4919–4926. [PubMed: 15256464]
38. Rahmani M, Yu C, Dai Y, Reese E, Ahmed W, Dent P, et al. Coadministration of the heat shock protein 90 antagonist 17-allylamino- 17-demethoxygeldanamycin with suberoylanilide hydroxamic acid or sodium butyrate synergistically induces apoptosis in human leukemia cells. Cancer Res. 2003; 63:8420–8427. [PubMed: 14679005]
39. Liu C, Sarkaria J, Allen C, Zollman PJ, James CD, Russell SJ, et al. Combination of oncolytic measles virus strains and radiation therapy has synergisitic activity in the treatment of glioblastoma multiforme. (Abstract 44). Mol Ther. 2006; 13(suppl 1):s19.
40. Sylwester A, Wessels D, Anderson SA, Warren RQ, Shutt DC, Kennedy RC, et al. HIV-induced syncytia of a T cell line form single giant pseudopods and are motile. J Cell Sci. 1993; 106(Part 3): 941–953. [PubMed: 8308076]
41. Eitzen G. Actin remodeling to facilitate membrane fusion. Biochim Biophys Acta. 2003; 1641:175–181. [PubMed: 12914958]
42. Singh I, Knezevic N, Ahmmed GU, Kini V, Malik AB, Mehta D. G{alpha}q-TRPC6-mediated Ca2+ Entry Induces RhoA Activation and Resultant Endothelial Cell Shape Change in Response to Thrombin. J Biol Chem. 2007; 282:7833–7843. [PubMed: 17197445]
43. Goldberg L, Kloog Y. A Ras inhibitor tilts the balance between Rac and Rho and blocks phosphatidylinositol 3-kinase-dependent glioblastoma cell migration. Cancer Res. 2006; 66:11709–11717. [PubMed: 17178866]
44. Rittinger K, Walker PA, Eccleston JF, Smerdon SJ, Gamblin SJ. Structure at 1.65 A of RhoA and its GTPase-activating protein in complex with a transition-state analogue. Nature. 1997; 389:758–762. [PubMed: 9338791]
45. Gower TL, Pastey MK, Peeples ME, Collins PL, McCurdy LH, Hart TK, et al. RhoA signaling is required for respiratory syncytial virus-induced syncytium formation and filamentous virion morphology. J Virol. 2005; 79:5326–5336. [PubMed: 15827147]
46. Liu TS, Musch MW, Sugi K, Walsh-Reitz MM, Ropeleski MJ, Hendrickson BA, et al. Protective role of HSP72 against Clostridium difficile toxin A-induced intestinal epithelial cell dysfunction. Am J Physiol Cell Physiol. 2003; 284:C1073–C1082. [PubMed: 12490434]
47. Sastry SK, Rajfur Z, Liu BP, Cote JF, Tremblay ML, Burridge K. PTP-PEST couples membrane protrusion and tail retraction via VAV2 and p190RhoGAP. J Biol Chem. 2006; 281:11627–11636. [PubMed: 16513648]
48. Carsillo T, Traylor Z, Choi C, Niewiesk S, Oglesbee M. hsp72, a host determinant of measles virus neurovirulence. J Virol. 2006; 80:11031–11039. [PubMed: 16971451]
49. Okamoto T, Nishimura Y, Ichimura T, Suzuki K, Miyamura T, Suzuki T, et al. Hepatitis C virus RNA replication is regulated by FKBP8 and Hsp90. EMBO J. 2006; 25:5015–5025. [PubMed: 17024179]
50. Connor JH, McKenzie MO, Parks GD, Lyles DS. Antiviral activity and RNA polymerase degradation following Hsp90 inhibition in a range of negative strand viruses. Virology. 2007; 362:109–119. [PubMed: 17258257]
51. Dressel R, Grzeszik C, Kreiss M, Lindemann D, Herrmann T, Walter L, et al. Differential effect of acute and permanent heat shock protein 70 overexpression in tumor cells on lysability by cytotoxic T lymphocytes. Cancer Res. 2003; 63:8212–8220. [PubMed: 14678977]
52. Asea A, Kraeft SK, Kurt-Jones EA, Stevenson MA, Chen LB, Finberg RW, et al. HSP70 stimulates cytokine production through a CD14-dependant pathway, demonstrating its dual role as a chaperone and cytokine. Nat Med. 2000; 6:435–442. [PubMed: 10742151]

53. Peng KW, Facteau S, Wegman T, O'Kane D, Russell SJ. Noninvasive *in vivo* monitoring of trackable viruses expressing soluble marker peptides. Nat Med. 2002; 8:527–531. [PubMed: 11984600]

54. Fulda S, Scaffidi C, Pietsch T, Krammer PH, Peter ME, Debatin KM. Activation of the CD95 (APO-1/Fas) pathway in drug- and gamma-irradiation-induced apoptosis of brain tumor cells. Cell Death Differ. 1998; 5:884–893. [PubMed: 10203687]

55. Nakamura T, Peng KW, Vongpunsawad S, Harvey M, Mizuguchi H, Hayakawa T, et al. Antibody-targeted cell fusion. Nat Biotechnol. 2004; 22:331–336. [PubMed: 14990955]

56. Liu C, Musch MW, Sugi K, Walsh-Reitz MM, Ropeleski MJ, Hendrickson BA, et al. Proapoptotic, antimigratory, antiproliferative, and antiangiogenic effects of commercial C-reactive protein on various human endothelial cell types *in vitro*: implications of contaminating presence of sodium azide in commercial preparation. Circ Res. 2005; 97:135–143. [PubMed: 15976313]

57. Ren XD, Kiosses WB, Schwartz MA. Regulation of the small GTP-binding protein Rho by cell adhesion and the cytoskeleton. EMBO J. 1999; 18:578–585. [PubMed: 9927417]

58. Servotte S, Zhang Z, Lambert CA, Ho TT, Chometon G, Eckes B, et al. Establishment of stable human fibroblast cell lines constitutively expressing active Rho-GTPases. Protoplasma. 2006; 229:215–220. [PubMed: 17180504]

59. Qiu RG, Chen J, McCormick F, Symons M. A role for Rho in Ras transformation. Proc Natl Acad Sci USA. 1995; 92:11781–11785. [PubMed: 8524848]

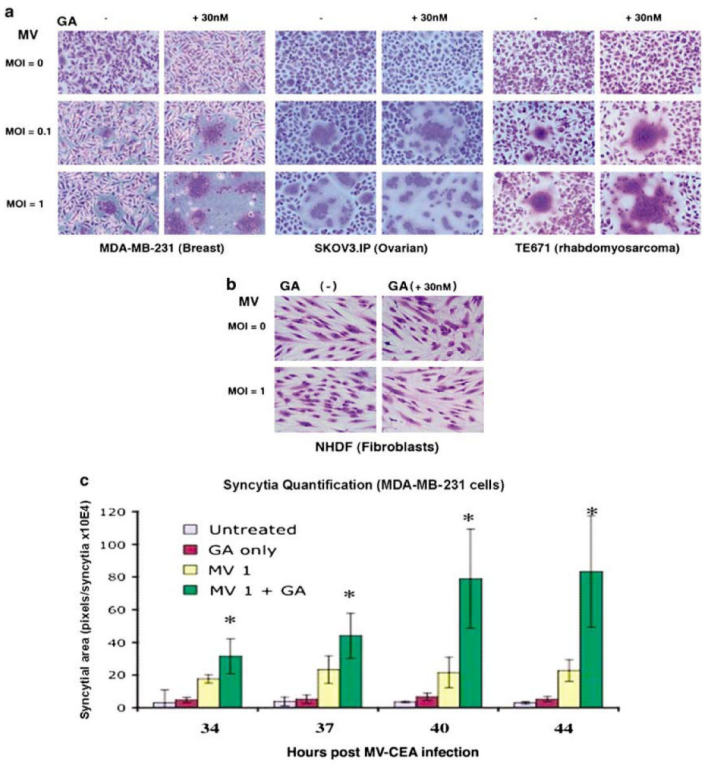


**Figure 1.**

(**a**) Cytopathic effect following MV-CEA/geldanamycin (GA) combination treatment. Addition of GA (30 nM), 24 h after infection with MV-CEA resulted in significant increase in cell fusion and cytopathic effect in different tumor cell lines (MDA-MB-231-breast; SKOV3.IP-ovarian; and TE671-rhabdomyosarcoma) as compared to virus alone. Images were obtained 48 h after MV-CEA infection. (**b**) MV-CEA/GA treatment at the same viral doses/concentration resulted in no cytopathic effect against nontransformed cells such as normal human dermal fibroblasts (NHDFs). (**c**) The syncytial area size was analyzed using NIH software. There was statistically significant increase in the syncytial area, when the measles virus infection was combined with GA treatment, as compared to measles virus infection alone (asterisk (*) denotes statistical significance).

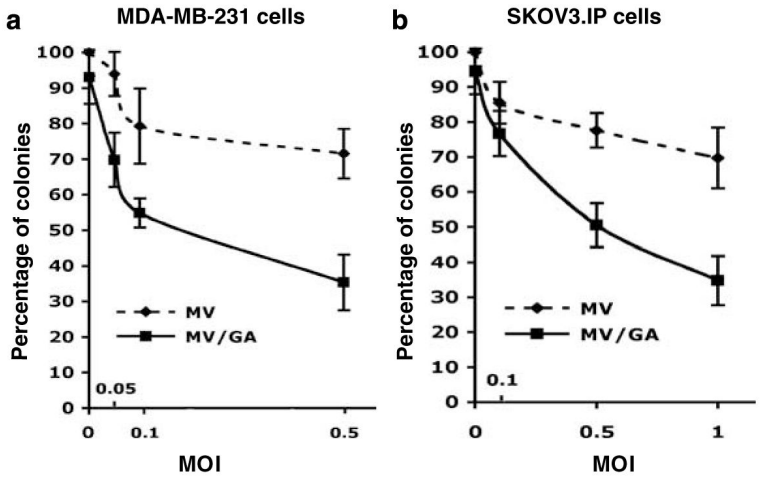


**Figure 2.**

Clonogenic assay of MV/geldanamycin (GA)-treated MDA-MB231 and SKOV3.IP cells. Significant decrease in colony formation was observed in the MV-CEA/GA group as compared to either single-agent MV-CEA treatment in comparable multiplicities of infection (MOIs), or single-agent GA treatment (30 $n_M$) in MDA-MB-231 (**a**) and SKOV3.IP (**b**) cells. Colony formation following treatment with single-agent GA corresponds to MOI=0 in the MV/GA curve.

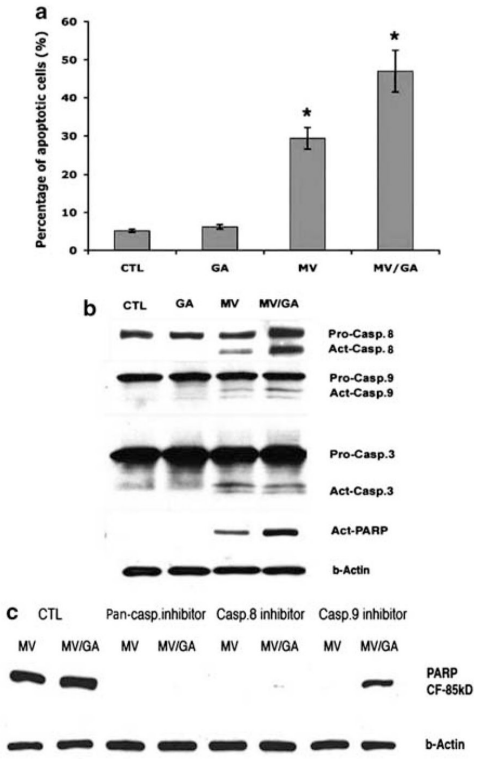


**Figure 3.**

Assessment of apoptosis in MV/geldanamycin (GA)-treated MDA-MB-231 cells (**a**) Quantification of apoptosis was performed using DAPI (4,6-diamidino-2-phenylindole) staining in MV-CEA/GA-treated MDA-MB-231 cells. Apoptotic cells were identified by condensation and fragmentation of the nuclei. Increase of apoptotic cells were observed in the MV-CEA and MV-CEA/GA groups as compared to either GA (30 $n_M$) alone or untreated MDA-MB231 cells (asterisk (*) denotes statistical significance). (**b**) Western blot analysis for caspase-8, -9, -3 and poly(ADP-ribose) polymerase (PARP) (p85) in MV/GA-treated MDA-MB231 cells in cell lysates obtained at 30 h following MV infection. There was increase in cleaved caspase-8 and PARP in MV/GA-treated cells as compared to MV- or GA-treated cells, (**c**) complete inhibition of PARP cleavage in MV/GA-treated cells was observed after the addition of pan-caspase inhibitor, or caspase-8 inhibitor, but not caspase-9 inhibitor, indicating predominantly caspase-8-dependent activation of apoptosis in combination-treated cells.

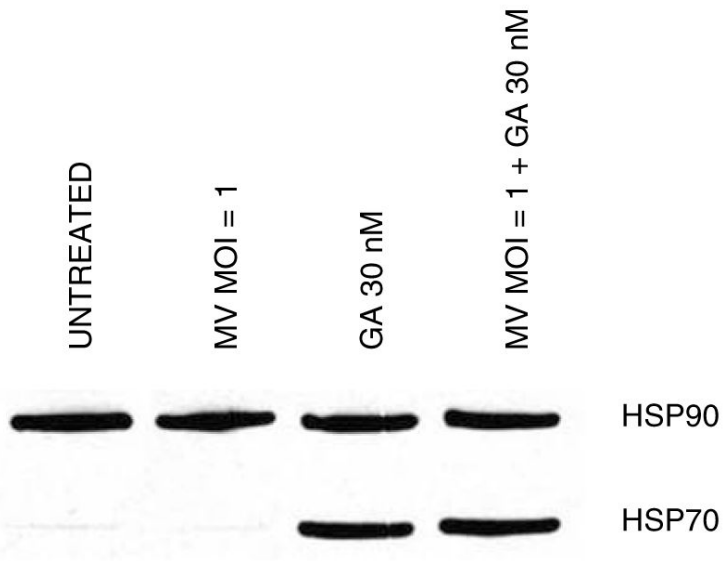


**Figure 4.**
Western immunoblotting of MDA-MB-231 cell lysates with heat shock protein 90 (HSP-90) or heat shock protein 70 (HSP70) antibody demonstrates increased HSP70 expression both in geldanamycin (GA) and MV-CEA/GA-treated cells. There is no difference in HSP70 levels between combination treated and single-agent GA treated cells.

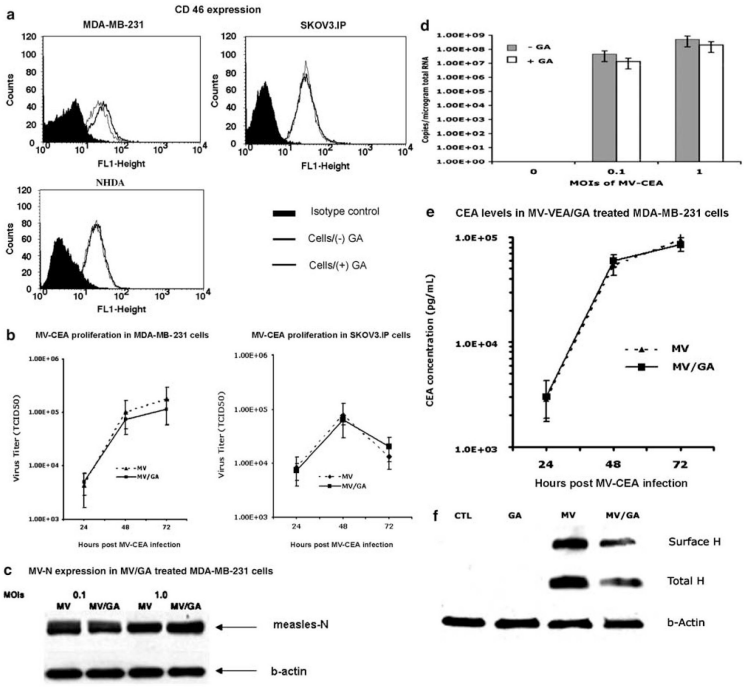


**Figure 5.**

(**a**) Fluorescence-activated cell sorting (FACS) analysis for CD46 expression, demonstrated no difference in measles virus receptor CD46 expression prior to and following geldanamycin (GA) treatment. (**b**) Assessment of viral replication in MV-CEA/GA combination-treated cells. One-step viral growth curves demonstrated that GA treatment did not increase the proliferation of MV-CEA in either MDA-MB-231 or SKOV3.IP cells. Both western immunoblotting (**c**), and QRT-PCR for measles virus N mRNA (**d**) showed no significant difference in N-protein expression in MV-CEA or viral genome copy number/GA combination-treated cells, as compared to MV-CEA treatment alone. (**e**) Similarly, there was no difference in CEA transgene expression between single-agent GA and combination-treated cells. (**f**) Total and cell surface hemaglutinin (H) protein expression levels were estimated by immunoblotting of cell lysates or of surface-biotinylated proteins immunoprecipitated with anti-FLAG antibody. There was no increase in H protein expression in combination-treated cells.

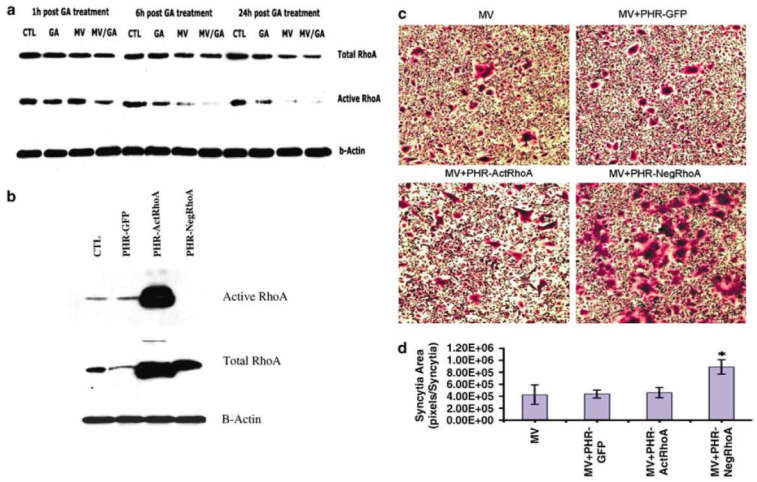


**Figure 6.**

(**a**) Immunoprecipitation assay for active RhoA and immunoblotting for total RhoA, showed decrease in RhoA activity starting at 6 h following geldanamycin (GA) treatment, which was more prominent in combination-treated cells. (**b**) Transduction of MDA-MB-231 cells with the PHR-NegRhoA lentiviral vector expressing a dominant-negative RhoA (MOI 10), completely eliminated RhoA-activity and significantly increased measles-induced fusion (**c**) and syncytial area (**d**) following measles virus infection. Lentiviral vectors expressing a constitutively active RhoA (PHR-ActRhoA) or GFP (PHR-GFP) were employed as controls. Asterisk (*) denotes statistical significance.